VELOCITY VARIATIONS WITHIN TONSON FAULT AREA, ARTHIT FIELD – NORTH MALAY BASIN

Nirut Tongpan

Department of Geology, Faculty of Science, Chulalongkorn University, Bangkok, 10330, Thailand
Corresponding author e-mail: tak.nirut@gmail.com

Abstract

Tonson fault trend is a major fault which is located in the northern part of Arthit field, North Malay Basin. Due to the large fault throw, the depth prediction is a challenge because of velocity variations within the fault blocks. Platform Alpha, which covers both upthrown and downthrown blocks of Tonson fault, results in a large error in depth prediction by using velocity modeling workflow, which uses only nearby well velocities and interpreted horizons. This study evaluated different velocity models for more accurate depth prediction and suggests appropriate workflow of velocity modelling for the area. The integration of well velocity, seismic velocity, structural control and pseudo velocity showed best statistical results for the depth prediction. This study recommends the use of pseudo velocity to improve the depth prediction in an area with high structural variation and sparsely located wells with velocity information. The velocity variation shows a conformable relationship with structure. Large vertical separation of Tonson fault causes significantly change in the velocity across upthrown and downthrown blocks. Velocities are low in the upthrown side and high in the downthrown side within the same stratigraphic interval. Moreover, the velocity trend also varies with the structural depth as high velocities were observed in deeper parts of the basin, whereas shallow parts have low velocities.

Keywords: Velocity model, Pseudo velocity, Tonson fault, North Malay Basin

1. Introduction

Arthit field is a petroleum field located in the northwestern margin of the North Malay Basin, Gulf of Thailand (Figure 1). This basin developed as an intra-cratonic basin by rifting in early Tertiary time. Structural styles in the basin were controlled by extensional mechanism along North-South and Northwest-Southeast oriented normal faults, that resulted a series of asymmetric half-grabens in the area.

Tonson fault trend is a major fault that is located in the northern part of Arthit field. Due to the large fault throw along this fault, the depth prediction is a challenge because of significant variation of velocities within the different fault blocks.

Petroleum development area of drilled platform Alpha (Figure 2), which covers both upthrown and downthrown blocks of Tonson fault has difficulty in velocity modeling for depth conversion. The depth prediction in this platform has shown a large error from the velocity modeling workflow which uses calibrated time-depth functions from nearby exploration wells that have check shot data and the structural conformance control from interpreted horizons. This velocity model results in a large error for depth prediction especially in downthrown block. This error is more prominent, when there is no velocity control point available in downthrown block (Figure 3).

This study attempted different workflows for velocity modeling and tested the suitability of each model by applying different statistical analysis. The best workflow is suggested for future use.

1.1 Objective

The main objectives of the study are

1. To evaluate various workflows of velocity

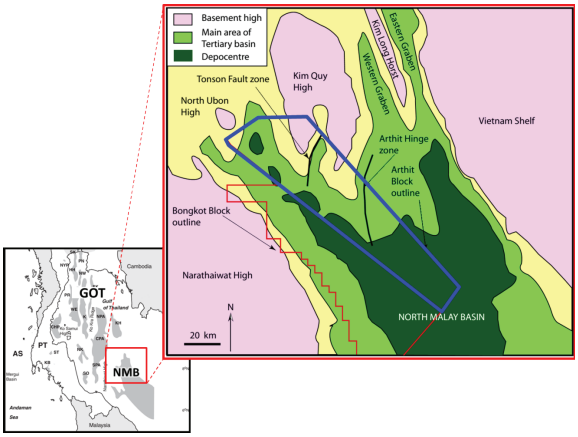

Figure 1. Location map of Arthit field (modified from Morley, and Racey, 2011)

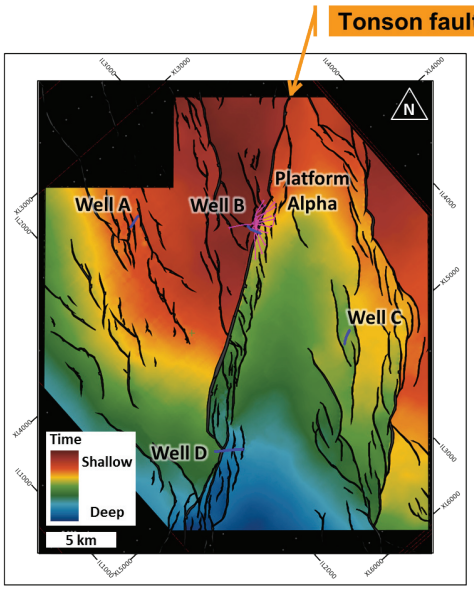

Figure 2. Location map of platform Alpha (pink wells) and the nearby exploration wells of well A, B, C, and D (blue wells), displayed on horizon H44

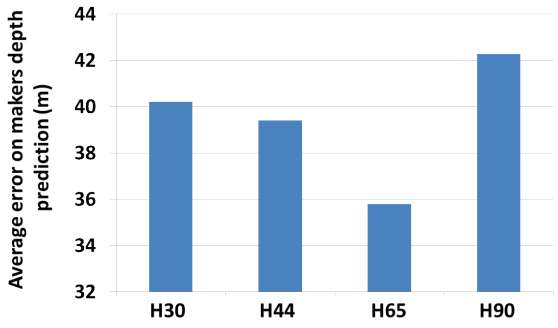

Figure 3. Average error on marker depth prediction of the platform Alpha's wells for markers H30, H44, H65 and H90

modeling and to suggest an appropriate workflow for accurate depth prediction for both sides of fault block.

2. To understand velocity variations along different geological setting in the area.

1.2 Geological background

Arthit field is located in the northwestern margin of the North Malay Basin, Gulf of Thailand. Based on the geological information, this basin developed as an intra-cratonic basin by rifting in early Tertiary time. Structural styles in the basin were controlled by extensional mechanism along North-South and Northwest-Southeast oriented normal faults, that resulted in a series of asymmetric half-grabens (Morley, and Racey, 2011).

Sediments supplied into the basin were both marine and non-marine deposits during rifting period. Formation 0 was deposited during Late Eocene to Late Oligocene in alluvial and lacustrine depositional environment during syn-rift period. Formation 1 was deposited during Late Oligocene to Early Miocene in alluvial outwash plain depositional environment unconformably over Formation 0. Formation 2 was deposited during Early to Middle Miocene unconformably overlies Formation 1. Formation 2 depositional environments comprise overall retrogradational fluvial environment that grade to estuarine environment in the southward area. (Figure 4)

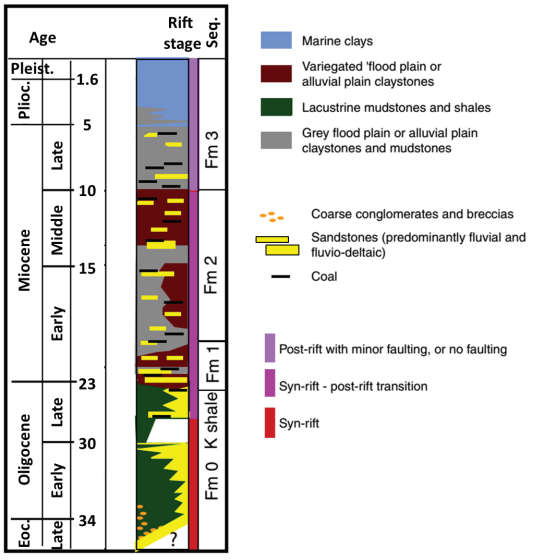

Figure 4. Stratigraphic Column of Arthit field, North Malay Basin (modified from Morley, and Racey, 2011)

2. Database and methodology

2.1 Database

A 3D Seismic data set was acquired covering Arthit field in 1998, survey lines orientation is SE-NW using a dual source and six streamer configurations. In 2012, seismic was reprocessed up to pre-stack time migrated level. The 3rd pass velocity analysis in the reprocessing provides RMS stacking velocity with a resolution of 50m by 50m, which will be used as the seismic velocity controlling input for the velocity modeling.

Well data from 4 exploration wells and 16 wells in platform Alpha were used in this study including well log, geological markers, and VSP/Check shot (only in exploration wells). Four regional horizons of H30, H44, H65, and H90 and also faults were provided as the structural interpretation in this study. The details of available data for the project are mentioned in Table 1.

Data type	Details
Seismic	3D PSTM seismic from line 1480 to 3840, trace from 3020 to 5960
Velocity	RMS stacking velocity
Check shot	4 exploration wells
Horizon	4 regional horizons of H30, H44, H65, and H90
Well data	From 16 wells in platform Alpha, 15 well picks at H30 surface 16 well picks at H44 surface 15 well picks at H65 surface 9 well picks at H90 surface

Table 1. The details of available data for the study

2.2 Methodology

The methodology is comprised of 5 steps as mentioned below.

Step1: Observed overall trend and relationship of velocity and geological setting

- Observed velocity trend and anomalous area from seismic velocity data
- Observed geological setting trend using conventional seismic data and generated seismic attribute data such as coherence analysis, which provide the possible structural trend through the discontinuity of seismic signal that changed by difference acoustic properties of surrounding matter
- Correlated the velocity trend associated with geological trend, in order to define the possible geological factors that effect to velocity

Step 2: Seismic to well correlation

- Created synthetic seismogram calibration to fit the geological properties derived from well log data with seismic data
- Four exploration wells were calibrated using sonic and density logs for acoustic impedance calculation. Well check shot data was applied as reference curve to calibrate the Time-depth curve derived from the sonic log. The reflection coefficient series was convolved with extracted wavelet, which derived statistically from seismic data along the well in the target zone.
- Then, generated synthetic trace was calibrated with composite trace extracted from conventional seismic around well bore. Major reflection coefficients were used as a key to match with strong seismic reflections to adjust time-depth relationship through stretch and squeeze process.
- Resulted in calibrated time-depth and velocity trend, which was suitable to be used in velocity modeling for this seismic data.

Step 3: Observed geological pattern of each factor from the regional horizon and fault interpretation, such as

- Observed variation and trend of depth from time structural map
- Observed variation and trend of thickness from isopach map
- Also observed the relationship between the variations and Tonson fault evolution

Step 4: Created and validated the velocity models with difference factor control inputs in order to see how the velocity model character changed due to each controlling input.

- Created 5 models of various inputs including

1. Well velocity from calibrated time-depth functions of 4 exploration wells that have check shot data
2. Structure control from 4 regional interpreted horizons of H30, H44, H65, and H90

3. Seismic velocity, derived from RMS stacking velocity data by Dix's conversion that calculated the interval velocity from RMS (Figure 5)
4. Platform downthrown wells average pseudo velocity, derived from the average trend of pseudo velocity in all platform downthrown wells using the relationship of seismic marker time and actual maker depth from well result (Figure 6). This additional velocity point will be placed at the platform downthrown center area.
5. All individual wells pseudo velocity derived from all wells in the study and placed at each well location.

The summary of various inputs data for each velocity model is mentioned in Table 2

- Tested the validation of velocity models using
1. Platform well marker prediction (well pick report)

The comparison between the actual marker depth and the calculated marker depth from time-depth conversion in each model was used to justify the proper of velocity modeling. Following the same time point where well trajectory intersects with horizon, difference time-depth conversion in each model will give difference marker depth prediction. As a result, a better velocity model should provide a smaller difference between the actual marker depth and the predicted.

2. Uncertainty analysis (drop-out analysis)

The measure of the uncertainty in the velocity model in this analysis derived from a tested model that removed one well data (pick and time-depth function) at a time and computed new model with remaining data. Then the new calculated marker depth will be compared with the actual depth to see the error as difference depth prediction. This analyzed result will define the confidence and accuracy of velocity model for the validation.

Step 5: Refer to the best-validated velocity model, interpret the relationship of velocity characteristics pattern associated with variation of each geological factors in the study area.

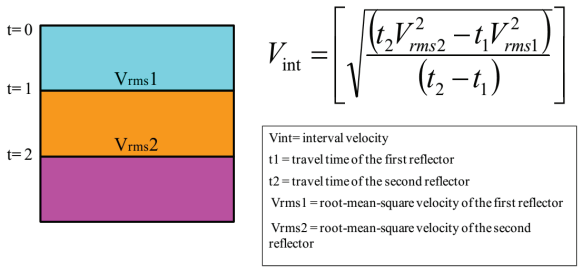

Figure 5. Calculation of interval velocities from RMS (modified from Dix, 1955 and Sheriff, 1991)

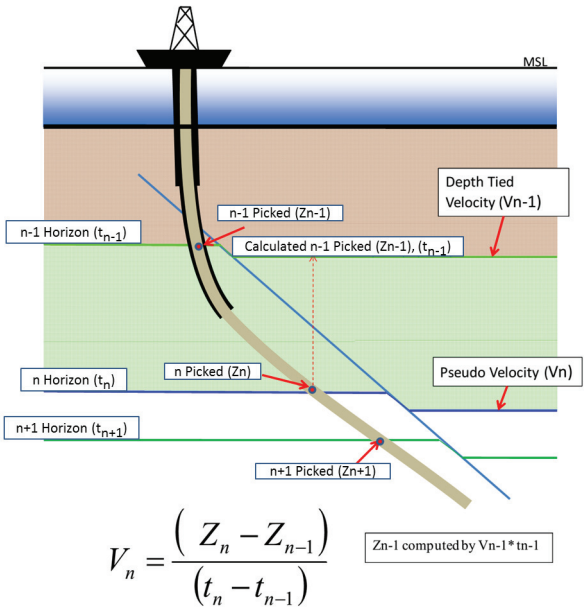

Figure 6. Calculation of pseudo velocities by using horizon and well picks (modified from Geena, 2012)

	Model 1	Model 2	Model 3	Model 4	Model 5
Well velocity from calibrated time-depth function in 4 exploration wells with checkshot data	✔	✔	✔	✔	✔
Structural from 4 horizons		✔	✔	✔	✔
Seismic velocity			✔	✔	✔
Downthrown well average pseudo velocity from *average* psudo velocity in platform downthrown wells *put as one well in center area				✔	✔
All individual well pseudo velocity from *all* pseudo velocity in all wells (exploration & platform well) *put in all individual wells					✔

Table 2. The summary of various input data for each velocity model

3. Result and discussion

3.1 Seismic velocity variation within different geological structures

The seismic velocities are aligned with geological structures as observed on the conventional seismic data and coherence attribute volume. Figure 7-9 show the seismic velocity pattern overlying on the seismic data, indicates the significant variation of velocity change associated with fault block boundary. This observation suggests that the structural setting is one of the major controlling factors of velocity character in this study area.

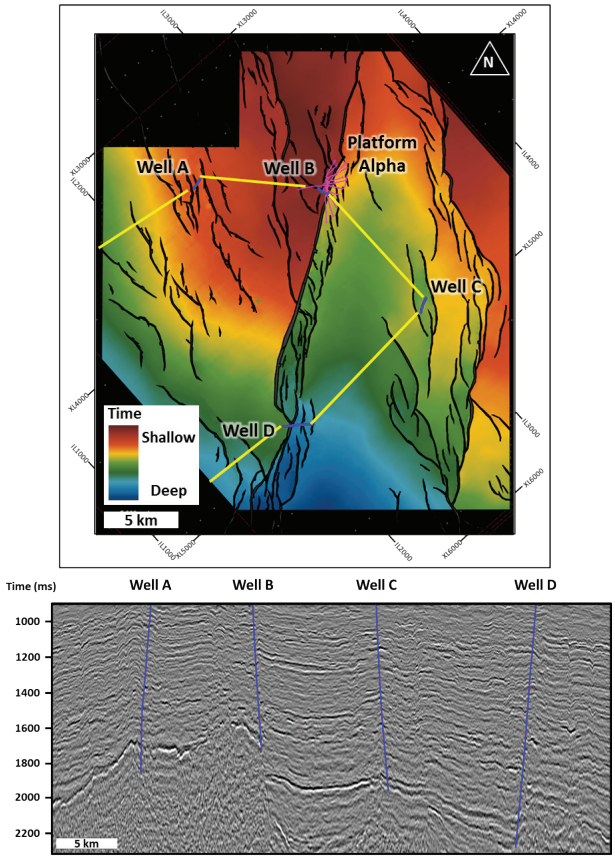

Figure 7. Seismic section along 4 exploration wells

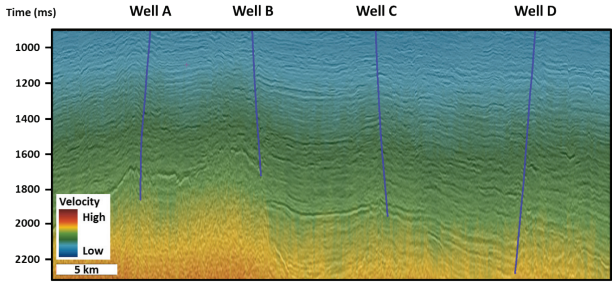

Figure 8. Seismic section along 4 exploration wells overlain by seismic velocity

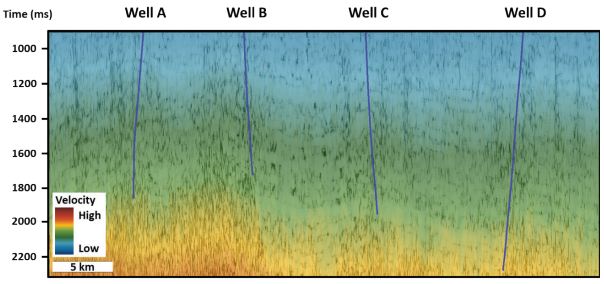

Figure 9. Seismic coherency attribute section along 4 exploration wells overlain by seismic velocity

3.2 Seismic to well calibration

As a result of synthetic calibration in 4 exploration wells, the correlation coefficient values between the synthetic trace and extracted trace from seismic data along well range show reasonable match (Figure 10). This process provides new calibrated time-depth function, which is more suitable to be used in velocity modeling. Plots of time-depth function (Figure 11) of 4 wells show the relative velocity trend of wells, result as shallower wells in upthrown block have a faster trend in comparative to deeper wells in the downthrown side.

The calibrated time-depth functions derived from synthetics were compared to raw check shot data to observe unreasonable values due to stretch-squeeze adjustment (Figure 12). According to the results, the adjusted velocities are in comparison with a raw check shot.

Interval velocities in four wells show two major velocity breaking. Below the top FM0 (H90), the interval velocity increases. Similarly below the top FM1 (H65), there is a general increase in interval velocity is observing in three wells (well A, B, and D) whereas well C does not show this pattern.

3.3 Structural variation in the study area

According to the seismic interpretation, this study area can be separated into two zones by major Tonson fault oriented in NNW-SSE direction. Large throw of Tonson fault created large vertical separation between upthrown and downthrown blocks and resulted in different

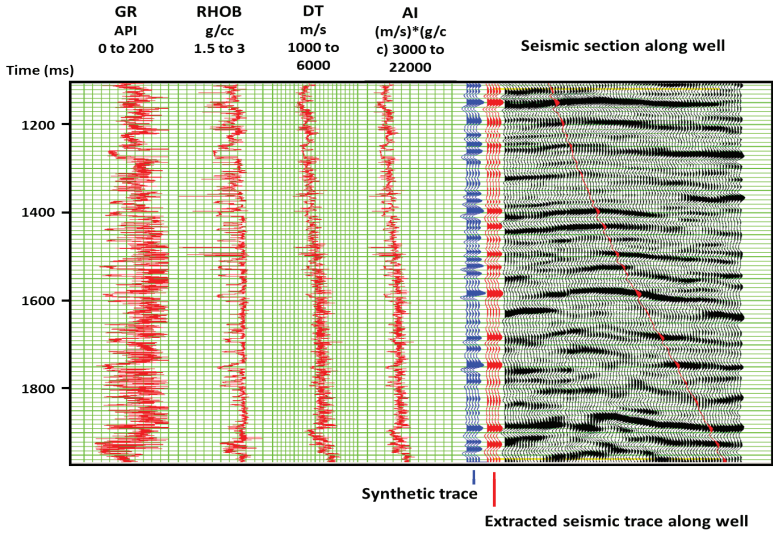

Figure 10. Well to seismic calibration result of well C. Blue trace represents the calibrated synthetic trace, and red trace represents conventional seismic trace along well.

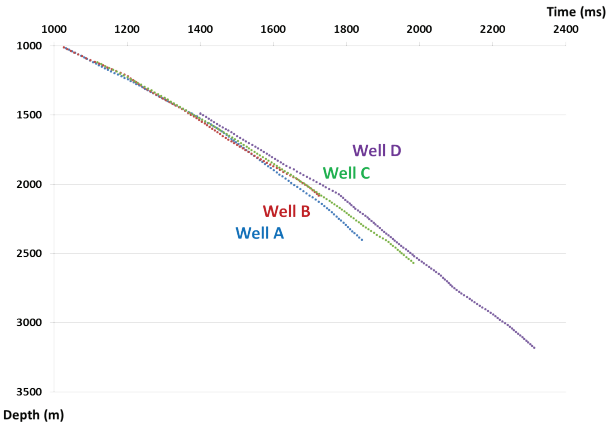

Figure 11. Calibrated time-depth plots of 4 exploration wells

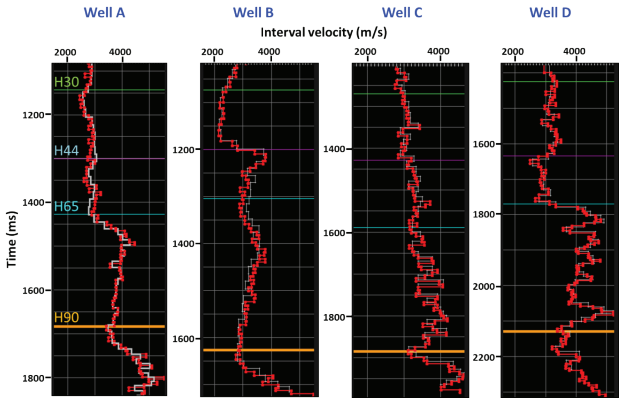

Figure 12. Interval velocity of 4 exploration wells overlain by 4 markers of H30 (green), H44 (purple), H65 (blue), and H90 (orange)

sedimentation rates in the same stratigraphic intervals between two sides of the block due to larger accommodation space in the downthrown side. This phenomenon caused thick deposition as seen in isopach maps and cross sections (Figure 13-16). The isopach maps and structural interpretation suggests that the deepest part of the basin is located in the southwestern part of the area.

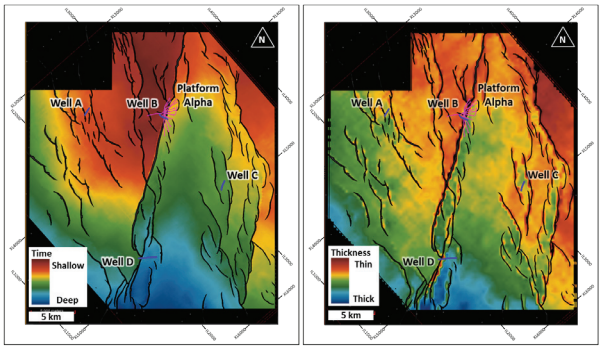

Figure 13. Time structural map (left) and Isopach map (right) of H30

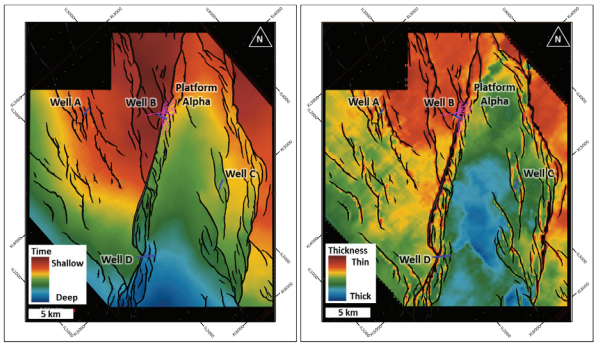

Figure 14. Time structural map (left) and Isopach map (right) of H44

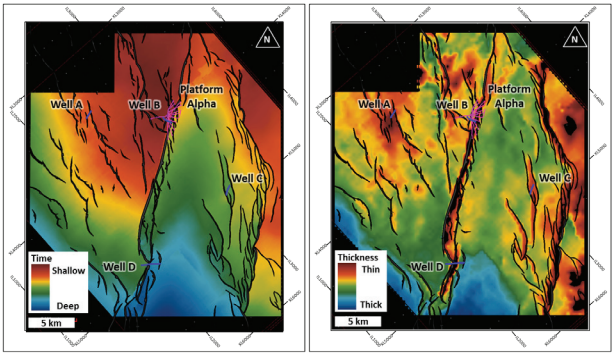

Figure 15. Time structural map (left) and Isopach map (right) of H65

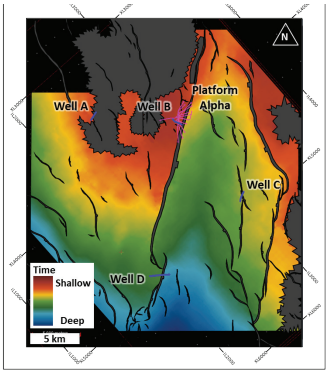

Figure 16. Time structural map of H90

3.4 Velocity modeling

Five velocity models of various inputs result in different velocity characters and also the effectiveness of marker prediction. The figures 17-21 of the overlying velocity models on seismic section provide the visualized variation of velocity pattern in each model. For the marker prediction effectiveness, the predicted marker depth was calculated using time-depth function in each model. Figure 22 shows the plots between predicted and actual marker depth following each model. The better accurate velocity model should give this plot point closer to the middle line, which means there is less error in prediction. Figure 23 and Table 3 also show the difference between the predicted and the actual depth of the picks.

Model 1

This model uses only calibrated time-depth function of 4 wells to generate the model. The marker prediction of platform wells using this model's conversion results showed average depth prediction errors range from 10 to 43 meters for four markers (Table 3). The velocity variation between each well is interpolated linearly through the radius of nearby wells. As the model input does not include the structural control, the velocity variation of this model is not parallel to the structural trend (Figure 17).

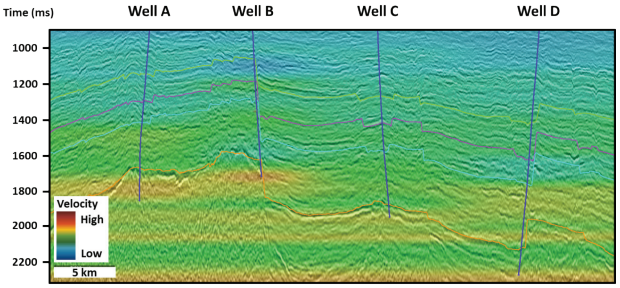

Figure 17. Seismic section overlain by velocity Model 1

Model 2

This model uses calibrated time-depth function of 4 wells and adds four horizons (H30, H44, H65, and H90) to guide the interpolation of well velocity along the structure. This additional input results in conformal alignment relationship between structural setting and velocity variation pattern (Figure 18). The depth prediction of markers by using this model gives a high error. The depth prediction average errors range from 36 to 42 meters for four markers (Table 33).

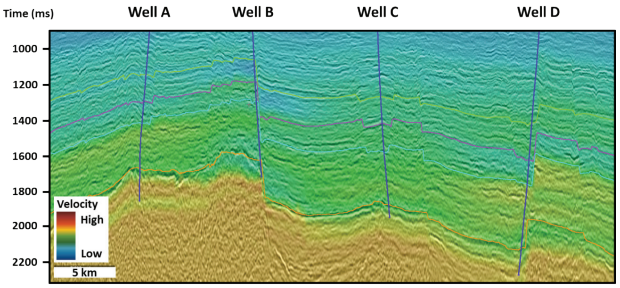

Figure 18. Seismic section overlain by velocity Model 2

Model 3

This model uses calibrated time-depth function of 4 wells, four horizons, and seismic velocity volume. The error in marker depth prediction from this model is reduced in comparison to model 2, as average errors range from 17 to 31 meters for four markers (Table 3). The velocity variation pattern in this model shows some detail lateral change within the stratigraphic intervals (Figure 19). This character

results from the additional input of seismic velocity which provides more detail in a lateral variation of velocities within the same stratigraphic interval through the controlling point from seismic velocity picked at 50m*50m interval.

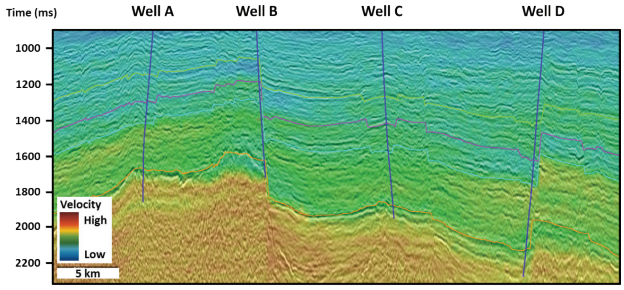

Figure 19. Seismic section overlain by velocity Model 3

Model 4

This model uses the calibrated time-depth function of 4 wells, 4 horizons, seismic velocity, and average pseudo velocity function derived from all pseudo velocity in platform downthrown wells. This function was computed because there was no check shot data available in platform downthrown block. The average pseudo velocity function was placed in the center of the platform in the downthrown block. The marker prediction result from this model is improved in comparison to model 3, as average errors range from 14 to 23 meters for four markers (Table 3). The addition of pseudo velocity control point changes the velocity in the downthrown block. This change can be observed along the downthrown side of the Tonson fault (Figure 20). In this model, the downthrown side has relatively higher velocity as compared to model 3. The improvement in the prediction of marker depth is caused by extra control point for the downthrown side.

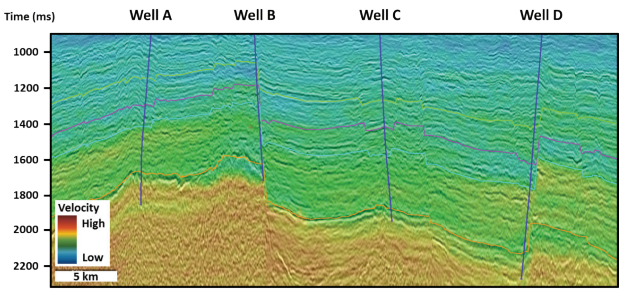

Figure 20. Seismic section overlain by velocity Model 4

Model 5

This model uses calibrated time-depth function of 4 wells, 4 horizons, seismic velocity, downthrown well's average pseudo velocity function, and all individual pseudo velocity from 20 wells in this model (4 exploration wells and 16 platform wells). The marker prediction from this model gives the best result in comparison to the other models, as it provides the average errors range from 3 to 10 meters for four markers (Table 3) as the result of the additional velocity control points which have been added at well locations.

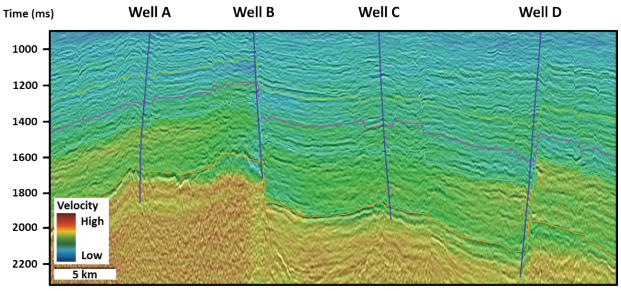

Figure 21. Seismic section overlain by velocity Model 5

As the result, marker prediction from the different models shows some change and improvement following the additional control points in the model. In this study, Model 5 gives the best marker prediction with the lowest error while Model 2 is the worst.

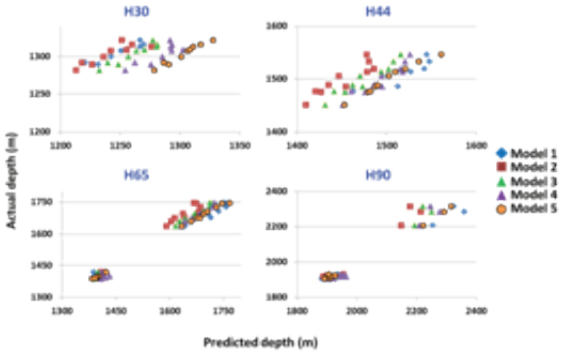

Figure 22. Plots between predicted and actual depth markers of 4 horizons from each model

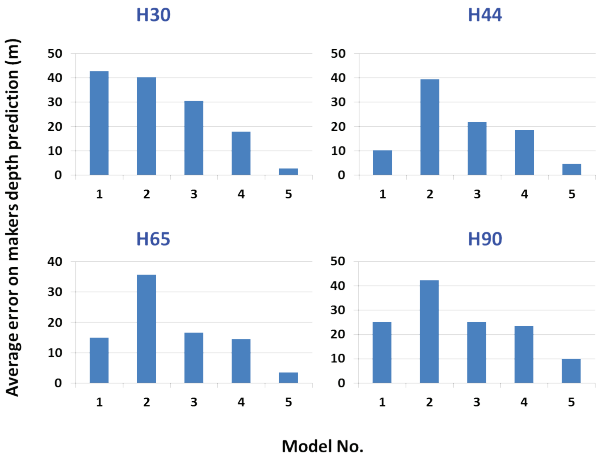

Figure 23. Average depth prediction error of 4 horizons from each model

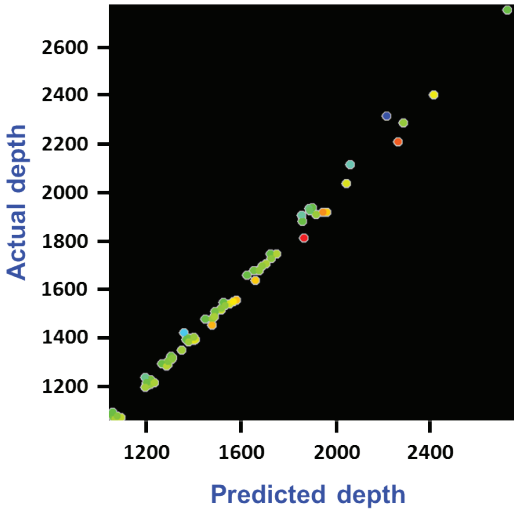

Figure 24. Plots of predicted and actual marker depth of drop-out analysis

	Model 1	Model 2	Model 3	Model 4	Model 5
Well velocity from calibrated time-depth function in 4 exploration wells with checkshot data	✔	✔	✔	✔	✔
Structural from 4 horizons		✔	✔	✔	✔
Seismic velocity			✔	✔	✔
Downthrown well average pseudo velocity from *average* psudo velocity in platform downthrown wells *put as one well in center area				✔	✔
All individual well pseudo velocity from *all* pseudo velocity in all wells (exploration & platform well) *put in all individual wells					✔
Average marker depth prediction error					
H30	42.87	40.22	30.66	17.93	2.76
H44	10.32	39.42	21.89	18.56	4.59
H65	15.07	35.79	16.60	14.45	3.63
H90	25.17	42.28	25.26	23.45	9.98

Table 3. Average depth prediction error of 4 horizons from each model

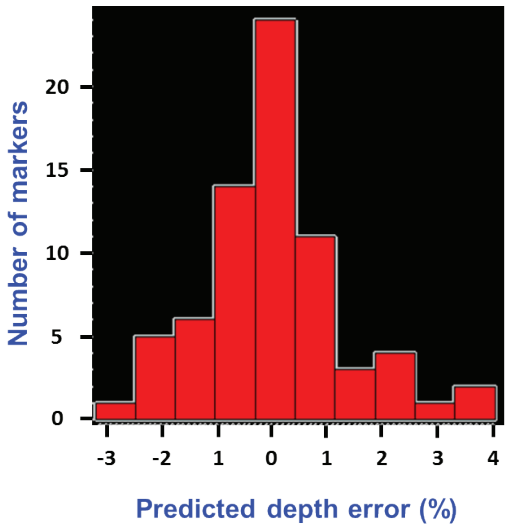

Figure 25. Maker depth prediction error histogram of drop-out analysis

Uncertainty analysis (drop-out analysis)

The uncertainty analysis was applied to the velocity Model 5, which predicted marker depths with lease error. In the drop-out test, the model 5 also shows acceptable results as the difference between predicted and actual marker depth is quite low as shown in Figure 24. The plots between these 2 values are close to the middle line, and also in Figure 25. The major population of maker prediction error in histogram shows value close to 0 percent.

3.5 Velocity maps

The velocity variation maps were extracted along four interpreted horizons (H30, H44, H65 and H90) by using the best model (Model 5). The study area is comprised of two major structural regions comprising of upthrown and downthrown blocks of Tonson fault.

The velocity map of H30 shows the variation of velocity change within two major structural regions (Figure 26). The upthrown block shows the slower trend of velocity variation in comparison to the downthrown block. Inside the fault blocks,

velocity follows a pattern along the structure. High velocities are observed in the deeper zone. The highest velocity in the study area was observed in the deepest part in the southwestern area of the downthrown block, while the lowest velocity was observed in the shallowest part in the northeastern area of the upthrown block. Similarly, velocity map for another surfaces such as H44, H65 and H90 (Figure 27 to 29) also show velocity variation along the structures. The velocities are different on two sides of the fault blocks and generally follow the pattern of the structural depth.

3.6 Discussion

Trend and variation of velocity characteristics in this study area have a conformal relationship with the structural setting. The major Tonson fault separates velocity trends into two regions by the large vertical separation between upthrown and downthrown block. This situation causes a significant change in the velocity trend and resulted in low velocity in upthrown side and high velocity in the downtrown side within the same stratigraphic interval. Moreover, the velocity trend also varies with the structural depth as evident by an occurrence of the high velocity in deeper areas which is maximum in the basin center.

Well velocity is one of the important inputs to the velocity model that controls the velocity pattern at well location area. These data were derived directly from check shot and well logs. Well velocity information can represent the velocity character only at the well location, or can be interpolated confidently to surrounding area if there is no lateral change in geological properties. However in this study area, there is a variation in structural and stratigraphic setting. Therefore, more control points are required to represent subsurface geological change.

Structural interpretation (horizons) has been used in the model to interpolate velocity pattern along the structural settings. This results in the parallel pattern of velocity variations along interpreted horizons.

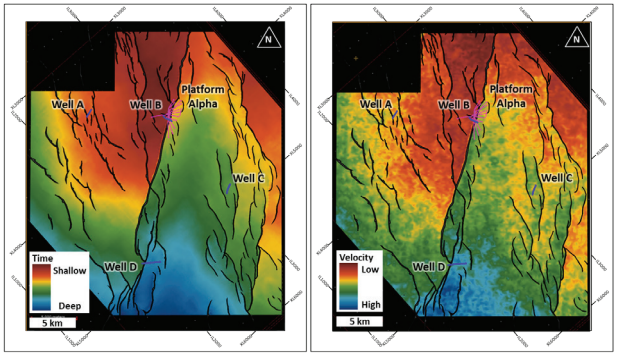

Figure 26. Time structural map (left) and Velocity map (right) of H30

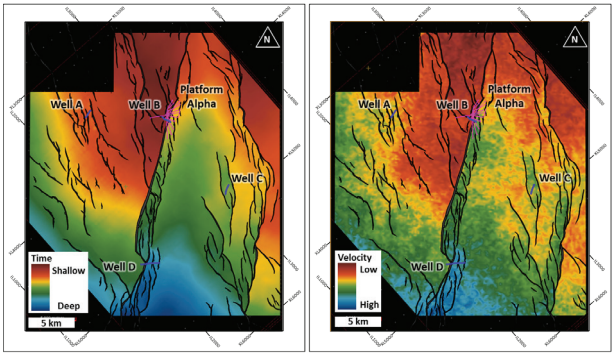

Figure 27. Time structural map (left) and Velocity map (right) of H44

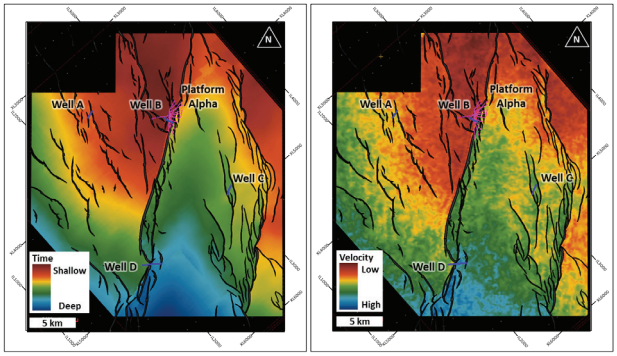

Figure 28. Time structural map (left) and Velocity map (right) of H65

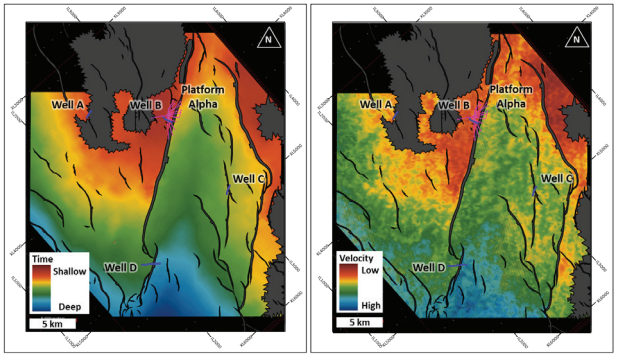

Figure 29. Time structural map (left) and Velocity map (right) of H90

Seismic velocity has been used in the model to give more information on lateral variation within the same stratigraphic interval.

All these three inputs seem to provide good controls for the velocity model, but still the depth prediction is not good especially in the downthrown side of the fault. The predicted depths in the downthrown block are shallower than the actual. Therefore, depth for downthrown blocks cannot be predicted by using velocities interpolated from upthrown block. The velocity difference between these two fault blocks may be related to the different compaction rates.

To input more control point to represent the accurate velocity for the downthrown block, the average pseudo velocity which was derived from all downthrown block wells was used. It improved the results for the depth prediction on downthrown side. However, it still has an error in the range of 14 to 23 meters. It may be due to the use of an average single velocity function which may not be a true representation of actual subsurface velocity. Therefore, to make the improvement, pseudo velocity function of all wells were added in the velocity model. The use of multiple pseudo velocity functions improved the prediction significantly and yielded the best results. The error for depth prediction reduces significantly i.e. in the range of 3 to10 meters.

Why Model 2 (which used well velocity and structure) results in larger error for depth prediction as compared Model 1 (which used only well velocity)? Generally by adding more control points, the velocity model should improve and predict depths more accurately. But in this case, the velocity Model 2 which used a structural control of stratigraphic intervals is not effective to predict depth in the downthrown block. The error in prediction may be related to lack of control points on the downthrown side near the well platform. The interpolation between well velocity functions is based on inverse distance weight (IDW) technique. The proposed well is located in the downthrown side and this well is close to the well with velocity information of upthrown side. Therefore, the wells of the platform on the downthrown side are more influenced by velocity function of a well in upthrown side.

According to the velocity modeling results of Model 2, structural control on stratigraphic intervals is not effective to interpolate the velocity variation in downthrown area due to lack of velocity control point near the platform at downthrown side.

In order to provide additional control point, this study used the average pseudo velocity functions computed from the time information of seismic markers and actual depth of corresponding markers in the well. For the pre-drilled work, this velocity function can be estimated from the pseudo velocity of nearby wells within the same major fault block. However, this function need to be used with awareness of possible lateral velocity changing within the same major fault block.

4. Conclusion

This study evaluated different velocity models by using various control inputs for the understanding of velocity characteristics in Tonson fault trend area and its relationship to the geological setting. The model, which showed best statistical results, uses well velocity, horizons, seismic velocity, an average pseudo velocity function in platform downthrown wells, and individual pseudo velocity in all wells.

Trend and variation of velocity characteristics in the study area have a conformal relationship with the structural setting. Large vertical separation of Tonson fault causes significant change in the velocity. There are low velocities in upthrown side and high velocities in the downtrown side within the same stratigraphic interval. Moreover, the velocity trend also variable with the structural depth as suggested by the occurrence of the high velocities in deeper areas.

The commonly used velocity model work-flow, which uses well velocity and structural control of

stratigraphic intervals cannot provide effective depth prediction in the downthrown side due to lack of control points. This workflow uses inverse distance weight technique for interpolation of the velocity between the wells. Therefore, if any proposed well on the downthrown side of the fault block is closer to the well on upthrown side, the velocity will be more influenced by the closer upthrown velocity control point. However, this computed velocity for the proposed well will not be true representative of geological setting. Therefore, extra control point is required to provide more realistic velocity control. Pseudo velocity function, derived from other wells on the downthrown side, can be used for this purpose. This study proposes to use the pseudo velocity function for more accurate depth prediction.

5. Acknowledgements

I would like to thank my supervisor Dr. Mirza Naseer Ahmad, for his valuable comments, warm support and excellent suggestions throughout my research project, and also Prof. Phillip Rowell, Mr. Angus John Ferguson, Prof. Joseph Lambiase, and Prof. John Warren for their knowledge through the Petroleum Geoscience Program. PTT Exploration and Production Public Company Limited is acknowledged for offering me the opportunity to use of their data. Landmark is acknowledged for providing academic licenses of software. I am very appreciate to my company supervisors; Mr. Kittipong Srisuriyon for giving me the chance to do this project, and also Petroleum Geoscience Program staffs for precious technical support throughout the year.

6. References

Dix, C.H., 1955, Seismic Velocity from surface Measurements; The Society of Exploration Geophysicists, v.20, p. 68-86.

Geena, S., 2012, An Integrated velocity modeling workflow to predict reliable depths in Trat field, Gulf of Thailand; Bulletin of Earth Sciences of Thailand, v.5, p.116-125.

Morley, C.K., and Racey, A., 2011, Tertiary stratigraphy, in M.F. Ridd, A.J. Barber, and M.J. Crow, eds., The geology of Thailand: Geological Society of London, p. 223-271.

Sheriff, R.E., 1991, Encyclopedic Dictionary of Exploration Geophysics, 3rd Edition: SEG Geophysical References Series 1, Tulsa, USA, p. 384.